Optics Communications 383 (2017) 191–196

Contents lists available at ScienceDirect

Optics Communications

journal homepage: www.elsevier.com/locate/optcom

Experimental demonstration of arbitrary waveform generation by a 4-bit photonic digital-to-analog converter

Bindong Gao, Fangzheng Zhang*, Shilong Pan

Key Laboratory of Radar Imaging and Microwave Photonics, Ministry of Education, Nanjing University of Aeronautics and Astronautics, Nanjing 210016, China

A R T I C L E I N F O

Article history:
Received 14 July 2016
Received in revised form
31 August 2016
Accepted 31 August 2016
Available online 12 September 2016

Keywords:
Digital-to-analog conversion
Microwave photonics
Waveform generation
Phase modulation
Optical pulse generation

A B S T R A C T

Arbitrary waveform generation by a serial photonic digital-to-analog converter (PDAC) is demonstrated in this paper. To construct the PDAC, an intensity weighted, time and wavelength interleaved optical pulse train is first generated by phase modulation and fiber dispersion. Then, on-off keying modulation of the optical pulses is implemented according to the input serial digital bits. After proper dispersion compensation, a combined optical pulse is obtained with its total power proportional to the weighted sum of the input digital bits, and digital-to-analog conversion is achieved after optical-to-electronic conversion. By properly designing the input bits and using a low pass filter for signal smoothing, arbitrary waveforms can be generated. Performance of the PDAC is experimentally investigated by establishing a 2.5 GSa/s 4-bit PDAC. The established PDAC is found to have a good linear transfer function and the effective number of bits (ENOB) reaches as high as 3.49. Based on the constructed PDAC, generation of multiple waveforms including triangular, parabolic, square and sawtooth pulses are implemented with the generated waveforms very close to the ideal waveforms.

1. Introduction

Arbitrary waveform generation has wide applications in modern radar, communication, and instrumentation systems. Traditionally, a waveform with programmable profile can be generated using an electrical arbitrary waveform generator, such as a direct digital synthesizer (DDS). However, the generated signal usually has a low frequency and the bandwidth is limited within several gigahertzes [1], which cannot meet the requirement in future high-speed and large-bandwidth systems. In addition, the signal quality is also limited by the large time jitter and severe electromagnetic interference (EMI) in pure electrical systems. To deal with these problems, photonic techniques have been proposed to generate microwave waveforms with the advantages of high frequency and large bandwidth. For example, by optical spectral shaping and frequency-to-time mapping, arbitrary waveforms with a bandwidth as large as tens of GHz can be generated [2,3]. Besides, specific waveforms such as triangular pulses and square pulses can be generated by manipulating the amplitude and phase of the harmonics generated by nonlinear electro-optical modulation [4–6]. The above schemes for waveform generation are realized by frequency-domain manipulations. The main limitation with such methods is either the small temporal aperture due to the limited resolution during optical spectral processing, or the poor flexibility generating only a few specific waveforms.

Photonic waveform generation by time-domain waveform synthesis is also proposed. The typical example is a signal generator based on a photonic digital-to-analog converter (PDAC), which can realize digital-to-analog conversion assisted by photonic technologies [7–15]. The prominent advantage of a PDAC is the superior flexibility, i.e., both the temporal duration and waveform profile can be arbitrarily designed. Besides, a PDAC is compatible with fiber communication and sensor networks, thus it has many special applications such as a label recognizer in all optical packet switching networks [7]. Therefore, the PDAC is a promising solution for future arbitrary waveform generators. According to the operation principle, a PDAC can work in parallel or serial mode. Most of the reported schemes belong to the parallel PDACs [8–12], which could be realized by intensity weighting and summing [8–10], coherent summing of phase modulated signals [11], or by nonlinear optical loop mirrors [12]. Parallel PDACs can take full advantage of the high speed electro-optic modulations and thus achieve a large sampling rate. However, the system is complicated considering the multi-channel parallel operations. Specifically, a parallel N-bit PDAC based on optical intensity weighting and summing requires N parallel channels. In this process, the parallel structure requires not only multiple laser sources and electro-optic modulators, but also precise synchronizations between the

* Corresponding author.
E-mail address: zhangfangzheng@nuaa.edu.cn (F. Zhang).

http://dx.doi.org/10.1016/j.optcom.2016.08.083
0030-4018/

multiple channels. As a result, the system has a high cost and complexity, especially for a high bit-resolution. On the other side, a serial PDAC allows a serial bit stream as the input. In serial PDACs, digital-to-analog conversion can be implemented by optical gating of delayed and weighted signals [13] or by pulse pattern recognition technique [14]. The requirement for multiple modulators is alleviated by applying serial modulation. While, in most of the previous serial PDACs, the modulated optical signal should still be split into multiple channels for further processing, such as to introduce different weights and time delays [13], or go through different pulse pattern recognition modules [14]. In [15], Peng et al. proposed a serial PDAC using time and wavelength interleaved optical pulses, where the intensity summation is realized based on fiber dispersion. This method implements serial modulation and summation in a single channel, thus the system is simplified compared with the previous serial PDACs. The system stability is also enhanced thanks to the compact structure. In the proof of concept experiment, the established PDAC has a bit resolution limited to 3. Although the operation principle of the PDAC is verified, the detailed properties of the PDAC (such as the effective number of bits) and the arbitrary waveform generation performance are not mentioned.

In this paper, we demonstrate an improved serial PDAC and perform a detailed experimental investigation of the PDAC as well as its application for arbitrary waveform generation. Different from that in [15], the intensity weighted, time and wavelength interleaved optical pulse train is generated by phase modulation with fiber dispersion. This scheme has the ability of generating very short optical pulses to avoid the inter symbol interference (ISI). Besides, the use of phase modulation is more power efficient compared with the intensity modulation applied in [15]. After intensity modulation according to the serial digital signal, the optical pulses at different wavelengths are temporally combined through fiber dispersion to implement optical intensity summation. In the experiment, the bit resolution of the established PDAC is extended to four and the sampling rate is 2.5 GSa/s. In addition to the transfer function of the PDAC, the effective number of bits (ENOB) of the PDAC is also investigated, which goes a further step compared with the work in [15]. Another expansion of the investigation here over the work in [15] is that, arbitrary waveform generation performance based on the established PDAC is evaluated through the generation of multiple waveforms including triangular, sawtooth, parabolic and square profiles.

2. Operation principle

Fig. 1 shows the schematic diagram of the proposed 4-bit serial PDAC. Four continuous wave (CW) lights at different wavelengths (λ_1, λ_2, λ_3, and λ_4) are generated by four laser diodes (LDs), of which the wavelength spacing is identical, i.e., $\Delta\lambda=\lambda_4-\lambda_3=\lambda_3-\lambda_2=\lambda_2-\lambda_1$. The four CW lights are combined by a wavelength division multiplexer (WDM) and then phase modulated at an electro-optic phase modulator (PM) driven by a RF signal having frequency f. After that, the phase modulated signals pass through a dispersion element (DE1). According to the optical pulse generation theory by phase modulation followed by fiber dispersion [16], four short optical pulse trains at different wavelengths are generated after DE1. Meanwhile, a time delay is introduced to the optical pulses at different wavelengths due to the fiber dispersion. By properly setting the wavelength spacing ($\Delta\lambda$) between adjacent channels to let

$$D_1\Delta\lambda = \frac{4n \pm 1}{4f} \tag{1}$$

where D_1 (ps/nm) is the dispersion of DE1 and n is an integer, a multi-wavelength pulse train with a repetition rate of $4f$ can be generated. Here, the overlap between adjacent pulses should be avoided by generating optical pulses with a small pulse width, which can always be satisfied by choosing an appropriate value of n. By tuning the power of the laser sources, the optical pulses at different wavelengths can be intensity-weighted to have a power ratio of 8:4:2:1 (point A in Fig. 1). Then, the time and wavelength

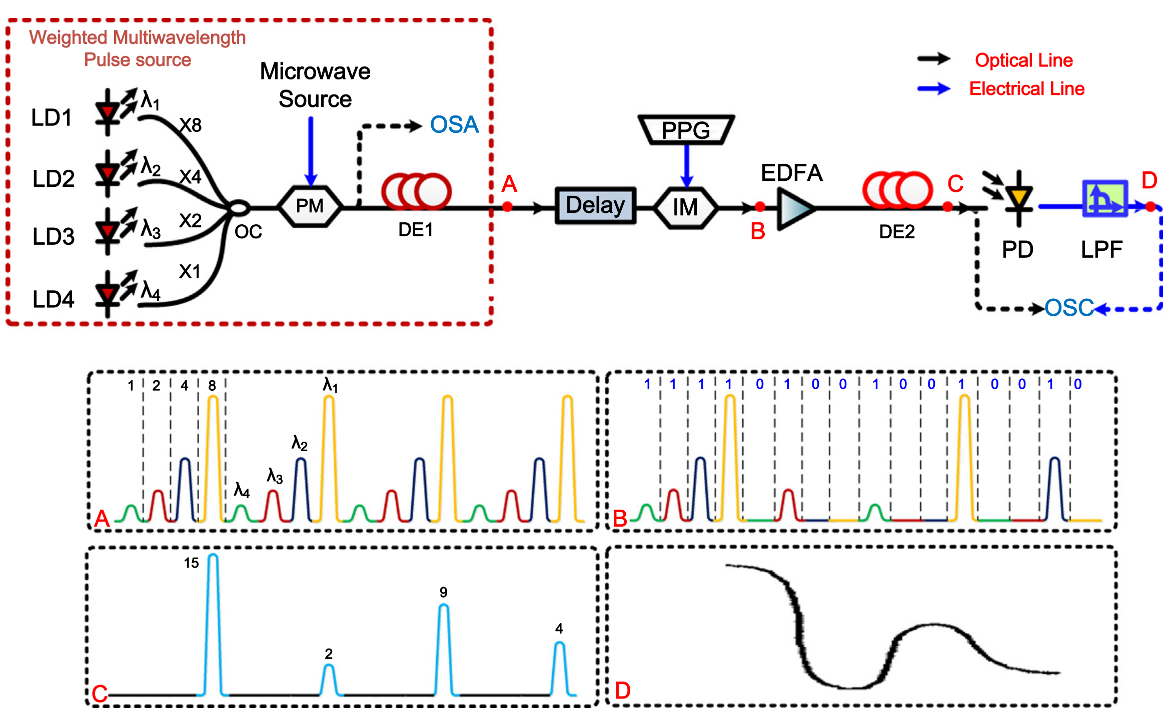

Fig. 1. Schematic diagram of the 4-bit PDAC. LD: laser diode, OC: optical coupler, PM: phase modulator, IM: intensity modulator; EDFA: erbium-doped optical fiber amplifier, PD: photodetector; EA: electrical amplifier, LPF: low pass filter, PPG: pulse pattern generator, OSA: optical spectrum analyzer, OSC: oscilloscope.

interleaved optical pulse train is on/off keying modulated by a Mach-Zehnder modulator (MZM) that is driven by a serial electrical digital stream with a bit rate of $4f$ bit/s. By adjusting an optical delay line, the digital signal can be synchronized with the optical pulse train so that the optical pulses with different weights can be modulated by the corresponding bits respectively (point B in Fig. 1). After the MZM, the modulated optical signal is fed to another dispersion element (DE2) having a dispersion of D_2 (ps/nm), which is properly chosen such that

$$(D_1 + D_2)\Delta\lambda = \frac{n}{f} \tag{2}$$

In this case, the time and wavelength interleaved optical pulses in a period would temporally coincide. The total optical power of each combined pulse would be proportional to the weighted sum of 4 consecutive bits from the input digital signal (point C in Fig. 1). After optical-to-electrical conversion at a PD, the output current is also proportional to the weighted sum of the input digital signals. As a result, a 4-bit digital-to-analog conversion with a sampling rate of f Sa/s is realized. To generate specific waveforms based on this PDAC, the input digital signals should be properly designed. In addition, an electrical low-pass filter (LPF) should be used after the PD to get a smooth waveform (point D in Fig. 1).

The main improvement in our system compared with the scheme in [15] lies in the optical pulse generation scheme. In [15], the time and wavelength interleaved optical pulses are generated by optical intensity modulation followed by a span of dispersion fiber. While in the proposed system, optical pulses are generated by phase modulation with fiber dispersion. The advantage of the scheme here is that it can generate very short pulses. This is helpful to avoid the inter symbol interference (ISI) that would otherwise deteriorate the PDAC performance. Besides, the use of phase modulation is more power efficient than intensity modulation. In the next part, an experimental investigation of the proposed PDAC is provided. Performance of the established PDAC is investigated in detail including the transfer function properties as well as the effective ENOB. Based on the established PDAC, the generation of multiple waveforms including triangular, sawtooth, parabolic and square profiles is demonstrated and evaluated.

3. Experimental investigation

In the experiment, a 2.5 GSa/s 4-bit PDAC is established. Here, the sampling rate is limited by the maximum bit rate of the pulse pattern generator (PPG). The four CW lights are generated by a 4-channel tunable laser source (EXFO IQS-636). The PM (EOSPACE AZ-AV5-40) has a bandwidth larger than 30 GHz and a half wave voltage of 4 V@1 GHz. It is driven by a 2.5 GHz RF signal generated from a microwave source (Agilent E8257D). The power of the RF signal applied to the PM is about 14 dBm. The wavelengths of the four lasers are set to 1550 nm, 1550.73 nm, 1551.46 nm and 1552.19 nm, respectively ($\Delta\lambda$=0.73 nm). A commercial dispersion compensation module (Coring DCM-Module) is used as DE1 with a dispersion of −682 ps/nm, and the induced time delay between two adjacent channels is −500 ps. In this case, the value of n is −1 and a minus sign is chosen in Eq. (1). After that, the optical pulse in a single wavelength is measured by an 80 GHz optical sampling oscilloscope (Agilent 86100C) and shown in Fig. 2(a), where the pulse has a full-width at half maximum (FWHM) of 20.4 ps and the pulse has a very small duty cycle of about 5%. This small duty cycle would effectively avoid the ISI between adjacent pulses. After adjusting the power of the laser sources, an intensity-weighted (8:4:2:1), time and wavelength interleaved optical pulse train is obtained. The measured waveform is shown in Fig. 2(b), where adjacent pulses are temporally separated by 100 ps. The spectrum of the optical pulses is measured by an optical spectrum analyzer (OSA, YOKOGAWA AQ6370C), as shown in Fig. 3(c). Then, the pulse train is modulated at a 10 Gb/s MZM (Lucent 2623NA), which is driven by a 10 Gb/s digital signal generated from the PPG (Anritsu MP1763C). An optical tunable delay line is used to ensure the pulse train and digital signal are synchronized in time domain. Following that, an 8-km single mode fiber (SMF) having a dispersion of +136 ps/nm is used as DE2. The time delay introduced by DE2 between two adjacent channels is +100 ps, thus the optical pulses in one period of $1/f$ are be temporally combined. A PD with a bandwidth of 10 GHz is followed to perform optical-to-electrical conversion.

To investigate the performance of the established PDAC, a 64-bit input digital signal with a pattern of '0000, 0001, 0010, 0011, …, 1111' is applied to generate samples corresponding to 16 digital levels from '0' to '15'. Fig. 3(a) shows the waveform of the 64 intensity modulated optical pulses before DE2. After DE2, 16 combined optical pulses corresponding to 16 different digital levels are obtained, as shown in Fig. 3(b). As can be seen, the 16 optical pulses in Fig. 3(b) are temporally separated by 400 ps, and the pulse power increases linearly as the samples increases. To analyze the transfer function of the PDAC, the power of each combined optical pulse is measured, as shown in Fig. 4, where a linear fit is also provided. According to the measured and fitted results in Fig. 4, the maximum integral nonlinearity (INL) and maximum differential nonlinearity (DNL) [17] is calculated to be 10.64% and 0.6393, respectively, indicating the established PDAC has a good linearity.

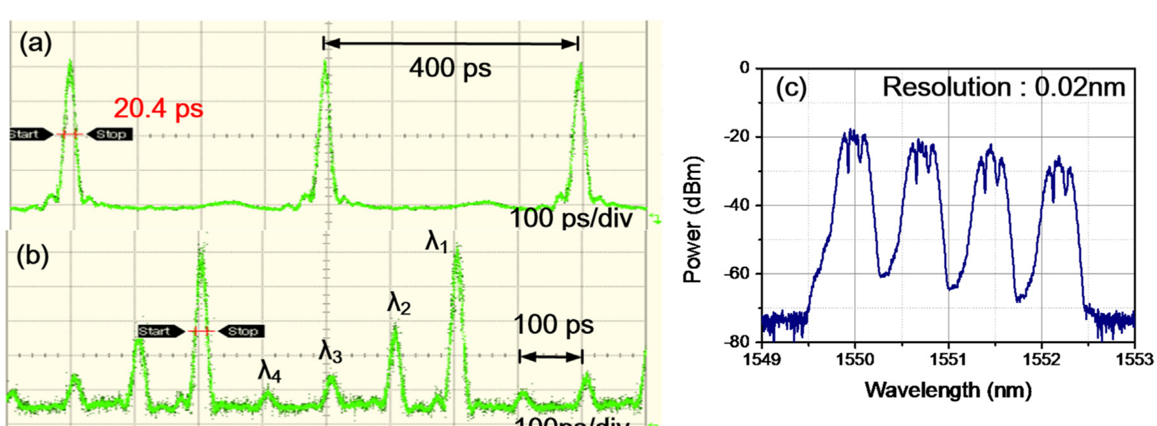

Fig. 2. (a) The generated optical pulse in a single wavelength, (b) the intensity weighted (8:4:2:1), time and wavelength interleaved optical pulses, and (c) the optical spectra of weighted pulse train.

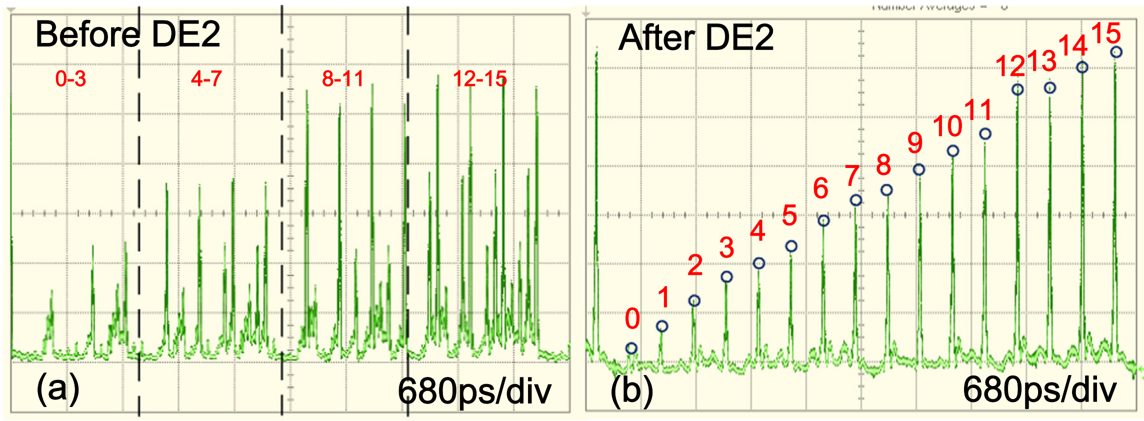

Fig. 3. Measured waveforms of the optical pulses (a) before and (b) after DE2 when a 64-bit digital signal is applied for level '0' to '15'.

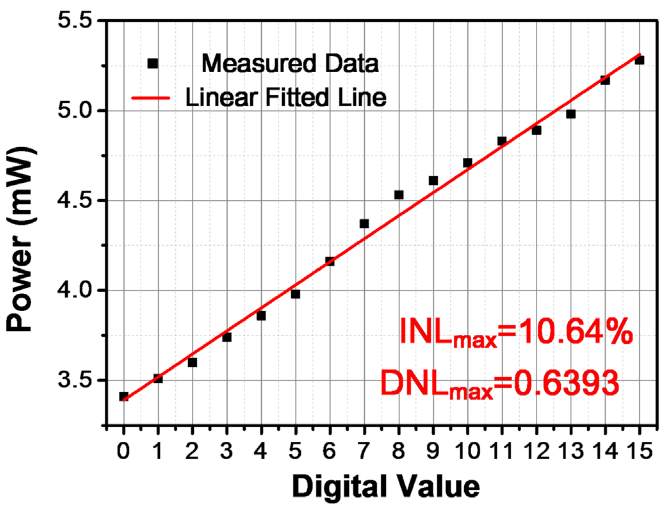

Fig. 4. Measured optical pulse power corresponding to 16 digital levels from 0 to 15, and its linear fit.

Then, the ENOB of the established PDAC is investigated by generating a single frequency cosine waveform. Using a set of designed 64-bit digital signal as the input, a 156.25 MHz cosine wave is generated by the PDAC. The waveform of combined 16 pulses after DE2 is shown in Fig. 5(a), where the targeted digital level in a period is '0, 1, 2, 5, 7, 12, 13, 14, 15, 14, 13, 12, 7, 5, 2, 1'. After the PD, an LPF with a bandwidth of 520 MHz is used. The obtained cosine wave is shown in Fig. 5(b). According to the measured cosine wave, a fitted ideal cosine wave is obtained, as shown in Fig. 5(c). By comparing the measured waveform with the fitted curve, the signal to noise and distortion ratio (SINAD) [17] is calculated to be 22.77 dB, and the ENOB [17] is 3.49, which is a good result for a 4-bit DAC at the sampling rate of 2.5 GSa/s.

Based on the established PDAC, arbitrary waveform generation can be implemented. Fig. 6 shows the results for generating triangular, parabolic, square and sawtooth pulses. In all the cases, the input digital signal has 64 bits in one period, indicating the repetition rate of the generated pulses is 156.25 MHz. For triangular wave generation, Fig. 6(a) shows the optical pulses after DE2 in one period, where the targeted digital levels for each pulse are noted. When using a 520 MHz LPF after the PD to smooth the waveform, the generated triangular pulse train is shown in Fig. 6(a). As can be seen, the generated waveform is very close to an ideal triangular pulse shape. To generate parabolic pulses, the targeted digital levels for each combined pulse after DE2 are shown in Fig. 6(b). Also using a 520 MHz LPF at the PD, the generated parabolic pulse train is shown in the figure. In Fig. 6(c), square pulses with a duty cycle of 50% are

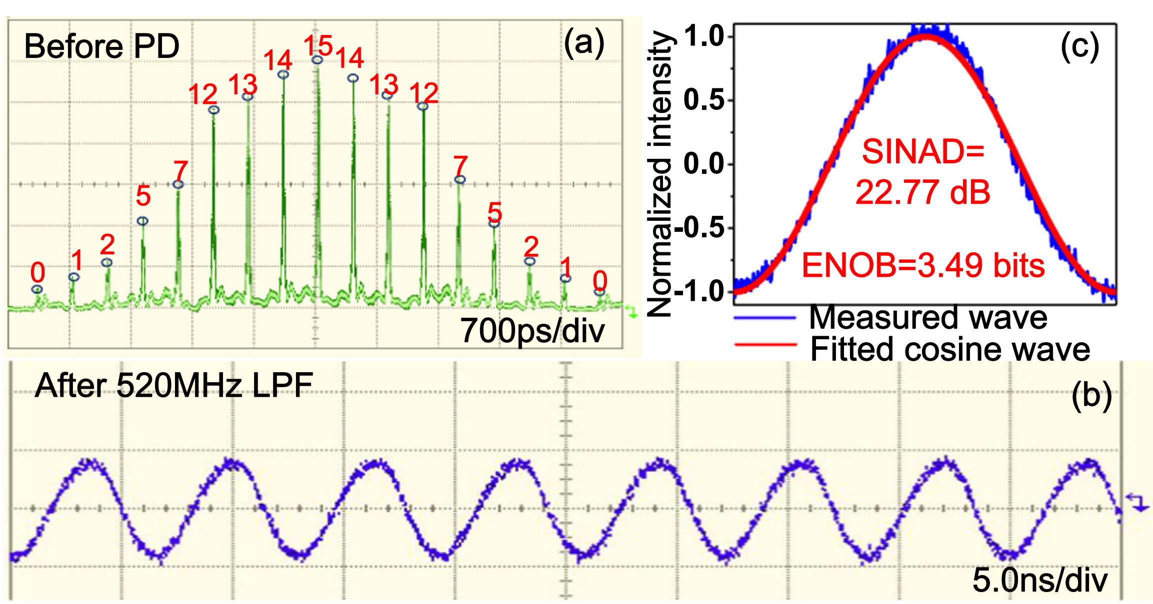

Fig. 5. Cosine waveform generation: (a) optical pulses after DE2, (b) the generated cosine wave after a 520 MHz LPF, and (c) comparison between the measured and fitted cosine wave.

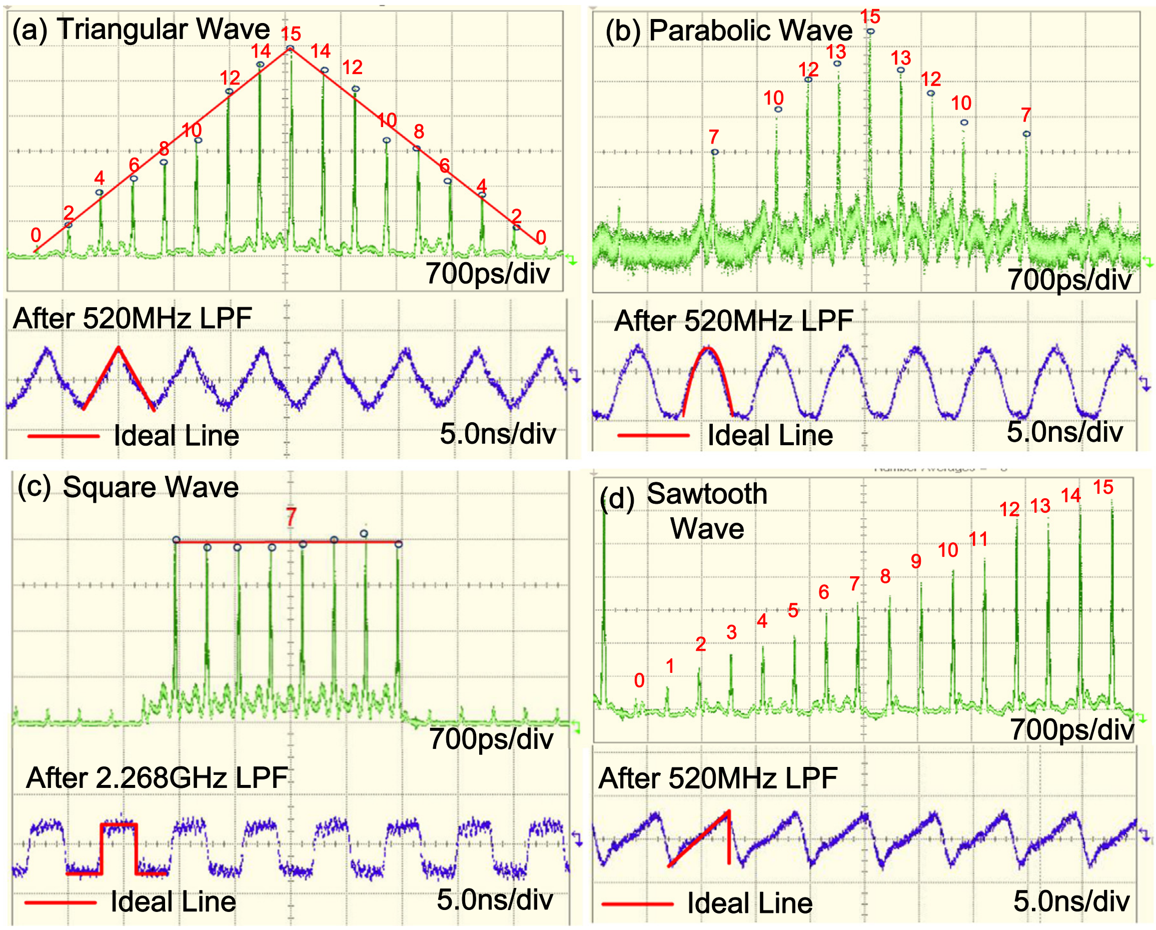

Fig. 6. Waveform generation based on the established PDAC: (a) triangular wave, (b) parabolic wave, (c) square wave and (d) sawtooth wave.

generated by composing 8 combined pulses at the same digital level in one period. To include the high frequency components after electrical-to-optical conversion, an LPF with a bandwidth of 2.268 GHz is used to get a smoothed square pulse train. In Fig. 6(d), by generating optical pulses with linearly increased power after DE2, an electrical sawtooth pulse train is generated after the PD and a 520 MHz LPF. Here, the non-ideal sharp edge of the sawtooth pulse is due to the bandwidth limitation of the LPF. To evaluate the quality of the generated waveforms, the root-mean-square error (RMSE) between the generated waveforms and the ideal waveforms is calculated [18], which is 9.058×10^{-4}, 1.0578×10^{-3}, 8.324×10^{-4}, and 7.231×10^{-3} for triangular parabolic, square and sawtooth pulses, respectively. The results can confirm that the generated waveforms are close to the ideal waveforms.

4. Discussion and conclusion

The bit-resolution of the PDAC is mainly determined by the duty cycle and extinction ratio of the generated optical pulses. In our experiment, the single-wavelength pulse train has a duty cycle of 5%, thus a possible bit-resolution of 20 can be achieved if twenty laser sources are used in the system. In addition, the extinction ratio of the time and wavelength interleaved optical pulse train also affects the bit-resolution, i.e., to construct an N-bit PDAC, the single-wavelength extinction ration should be larger than $10^*\log_{10}(2^N)$. Thus, an optical pulse train with a 30 dB extinction ratio could enable a bit-resolution of about 10.

In the experimental demonstration, due to the limitation of the PPG, the sampling rate of the established PDAC is limited to 2.5 GSa/s. In practical applications, the sampling rate is mainly determined by the on-off keying modulation speed of the IM. Currently, the modulation speed of an electro-optic modulator can reach 100 GHz [19], thus a sampling rate as high as 25 GSa/s can be achieved for a 4-bit PDAC. Assisted by temporal interleaving technique, the sampling rate can be further increased.

In summary, a serial PDAC system has been demonstrated and its performance for arbitrary waveform generation is investigated. The PDAC applies phase modulation and fiber dispersion to generate time and wavelength interleaved optical pulses with different weights. By on-off keying modulation of the optical pulses according to the input serial bit stream, and after proper dispersion compensation, digital-to-analog conversion is completed. In the experiment, the constructed 2.5 GSa/s 4-bit PDAC is found to have a good linearity and an ENOB as high as 3.49. Based on the PDAC, multiple waveforms including triangular pulses, parabolic pulses, square pulses and sawtooth pulses are successfully generated, and the good results can confirm its great potential in future arbitrary waveform generation applications.

Acknowledgements

This work was supported in part by the NSFC Program of China (61401201, 61422108, 61527820), the NSFC Program of Jiangsu Province (BK20140822), the Aviation Science Foundation of China (2015ZC52024), the Postdoctoral Science Foundation of China (2015T80549, 2014M550290), the open fund of Science and Technology on Monolithic Integrated Circuits and Modules Laboratory (20150C1404), and the Fundamental Research Funds for Central Universities.

References

[1] T.A. Schaffer, H.P.Warren, M.J. Bustamante, K.W.Kong, A 2 GHz 12-bit digital-to-analog converter for direct digital synthesis applications, in: Proceedings of the Technical Digest GaAs IC Symposium. 1996, pp. 61–64.
[2] J. Chou, Y. Han, B. Jalali, Adaptive RF-photonic arbitrary waveform generator, IEEE Photonics Technol. Lett. 15 (4) (2003) 581–583.
[3] F. Zhang, X. Ge, S. Pan, Background-free pulsed microwave signal generation based on spectral shapping and frequency-to-time mapping, Photonics Res. 2 (4) (2010) B5–B10.
[4] W. Liu, J. Yao, Photonic generation of microwave waveforms based on a polarization modulator in a Sagnac loop, J. Light. Technol. 32 (20) (2014) 3637–3644.
[5] F. Zhang, X. Ge, S. Pan, Triangular pulse generation using a dual-parallel Mach–Zehnder modulator driven by a single-frequency radio frequency signal, Opt. Lett. 38 (21) (2013) 4491–4493.
[6] X. Liu, et al., Photonic generation of triangular-shaped microwave pulses using SBS-based optical carrier processing, J. Light. Technol. 32 (20) (2014) 3797–3802.
[7] K. Sawada, H. Uenohara, High-speed optical label recognition technique using an optical digital-to-analog conversion and its application to optical label switch, J. Light. Technol. 28 (13) (2010) 1889–1896.
[8] A. Yacoubian, P.K. Das, Digital-to-analog conversion using electrooptic modulators, IEEE Photonics Technol. Lett. 15 (1) (2003) 117–119.
[9] M. Currie, J.W. Lou, Weighted, summing photonic digital-to-analog converter, Electron. Lett. 42 (1) (2006) 54–55.
[10] X. Yu, K. Wang, X. Zheng, H. Zhang, Incoherent photonic digital-to-analogue converter based on broadband optical source, Electron. Lett. 43 (19) (2007) 1044–1045.
[11] A. Leven, J. Lin, J. Lee, K.-Y. TU, Y. Baeyens, Y.K. Chen, A 12.5 Gsample/s optical digital-to-analog converter with 3.8 effective bits, in: Proceedings of the LEOS 2004, Puerto Rico, 2004, pp. 270–271.
[12] S. Oda, A. Maruta, All-optical digital-to-analog conversion using nonlinear optical loop mirrors, IEEE Photonics Technol. Lett. 18 (5) (2006) 703–705.
[13] T. Saida, et al., Integrated optical digital-to-analogue converter and its application to pulse pattern recognition, Electron. Lett. 37 (2001) 1237–1238.
[14] T. Nishitani, T. Konishi, H. Furukawa, K. Itoh, All-optical digital-to-analog conversion using pulse pattern recognition based on optical correlation processing, Opt. Express 13 (25) (2005) 10310–10315.
[15] Y. Peng, H. Zhang, Y. Zhang, M. Yao, Photonic digital-to-analog converter based on summing of serial weighted multiwavelength pulses, IEEE Photonics Technol. Lett. 20 (24) (2008) 2135–2137.
[16] B.J. Borthnik, H.R. Fetterman, High-speed photonically assisted analogy-to-digital conversion using a continuous wave multiwavelength source and phase modulation, Opt. Lett. 33 (19) (2008) 2230–2232.
[17] IEEE standard for terminology and test methods of digital-to-analog converter devices, IEEE Std 1658TM-2011, IEEE, New York, 2012.
[18] F. Zhang, B. Gao, P. Zhou, S. Pan, Triangular pulse generation by polarization multiplexed optoelectronic oscillator, IEEE Photonics Technol. Lett. 28 (15) (2016) 1645–1648.
[19] J. Khurgin, J. Kang, Y. Ding, Ultrabroad-bandwidth electro-optic modulator based on a cascaded Bragg grating, Opt. Lett. 25 (1) (2000) 70–72.